JOURNAL OF PROPULSION AND POWER
Vol. 17, No. 2, March–April 2001

Internal Plasma Properties and Enhanced Performance of 8-Centimeter Ion Thruster Discharge

John E. Foster* and Michael J. Patterson*
NASA John H. Glenn Research Center at Lewis Field, Cleveland, Ohio 44135

There is a need for a lightweight, low-power ion thruster for space science missions. Such an ion thruster is under development. In an effort to better understand the discharge performance of this thruster, a version of this thruster with an anode containing electrically isolated electrodes at the cusps was fabricated and tested. Discharge characteristics of this ring cusp ion thruster were measured without ion beam extraction. Discharge current was measured at collection electrodes located at the cusps and at the anode body itself. Discharge performance and plasma properties were measured as a function of discharge power, which was varied between 20 and 50 W. It was found that ion production costs decreased by as much as 20% when the two most-downstream cusp electrodes were allowed to float. Floating the electrodes did not give rise to a significant increase in discharge power even though the plasma density increased markedly. The improved performance is attributed to enhanced electron containment.

Nomenclature

$D_\perp$	=	cross-field diffusion coefficient
E_r	=	radial electric field
e	=	electron charge
M_i	=	ion mass
n_e	=	electron number density
n_0	=	plasma density
r	=	radial spatial coordinate
T_e	=	electron temperature
Γ_e	=	electron flux
Γ_i	=	ion current density
μ_e	=	electron mobility

I. Introduction

THERE is a need for a low-power (<0.5 kW), lightweight ion thruster for low-cost, small satellite space science missions.[1–3] Such a thruster is under development. This ion thruster, which generates an 8-cm-diam ion beam at the exit plane, is at present not optimized.[4] Because at low input powers the discharge power is a larger fraction of the total thruster power (sum of beam power and discharge power), minimizing the power required to generate the discharge plasma is particularly important. Indeed, the primary goal of ion thruster design is to optimize the tradeoff between discharge power and propellant efficiency. An essential aspect of optimizing the performance of an ion thruster is maximizing the discharge efficiency. The efficiency of an ion thruster discharge is characterized by the power required to produce a given beam current.[5] This parameter depends to a large degree on how well the energetic electrons are contained and utilized in the discharge chamber.

Containment of these energetic electrons is typically achieved by using strong permanent magnets in a multipole configuration. The ring–cusp magnetic circuit is one such configuration that has been used effectively for energetic electron containment.[5,6] This configuration consists of a series of magnet rings of alternating polarity. This arrangement produces a magnetic cusp at each magnet ring. In the ring–cusp configuration, electrons are prevented from reaching most of the discharge chamber surfaces due to strong magnetic field lines running nearly parallel to the chamber walls. Electrons with a sufficiently large velocity component parallel to the magnetic field are collected at the cusps; otherwise, they are reflected back into the discharge by the magnetic mirror force.[7] That most collection occurs at the center of the cusps (along a line that bisects the magnet ring) is readily observable as a discolored line on the magnets' surface or on the surface of the intervening material to which the magnets are affixed.

Plasma production was investigated in the discharge chamber of the 8-cm ring cusp ion thruster to obtain a better understanding of why the discharge losses are so large (>300 W/A at 100 W) and how to reduce them. The discharge investigation was carried out with four cusp electrodes, three ion wall probes, one langmuir probe, and an ion collecting grid, which replaced the high-voltage ion optics used for beam extraction. The cusp electrodes were used to measure the current distribution at the cusps as a function of operating condition. In addition, by electrically isolating one or more of these electrodes, it was possible to force the discharge current to collect in a specific cusp electrode configuration. This capability was used to externally vary and subsequently optimize discharge performance.

Note that data taken in this study are without ion beam extraction. It is well known that discharge properties change when there is beam extraction. Beam extraction tends to decrease the neutral concentration in the discharge chamber. Grid transparency to ions increases above the physical open area fraction during beam extraction, thereby increasing the effective ion loss rate to the beam.[8] This is due in part to the ions leaving the discharge at the Bohm velocity. Without beam extraction, ions are simply collected at the grid and reenter the discharge as neutrals. However, because the physical geometry of the discharge chamber and the magnetic circuit do not change, the trends measured in the case without beam extraction should be reflected under those conditions with beam extraction. In this respect, the studies performed without beam extraction should yield much insight into plasma production mechanisms that should be applicable to thrusters with beam extraction.

II. Experimental Apparatus and Approach

These experiments were conducted in a 41-cm-diam × 43-cm-long bell jar. The discharge chamber was mounted on a side port of the bell jar. The cryopumped bell jar maintained a background pressure in the high 10^{-6} Pa range. During discharge operation, the bell jar pressure never rose above 6×10^{-3} Pa.

A cross section of the 8-cm ion thruster's discharge chamber is shown in Fig. 1. The discharge chamber is cylindrically symmetric. The discharge chamber, which consists of a conical section

Received 5 January 2000; revision received 24 May 2000; accepted for publication 2 June 2000.

*Aerospace Engineer, Onboard Propulsion and Power, MS 301-3, 21000 Brookpark Road. Member AIAA.

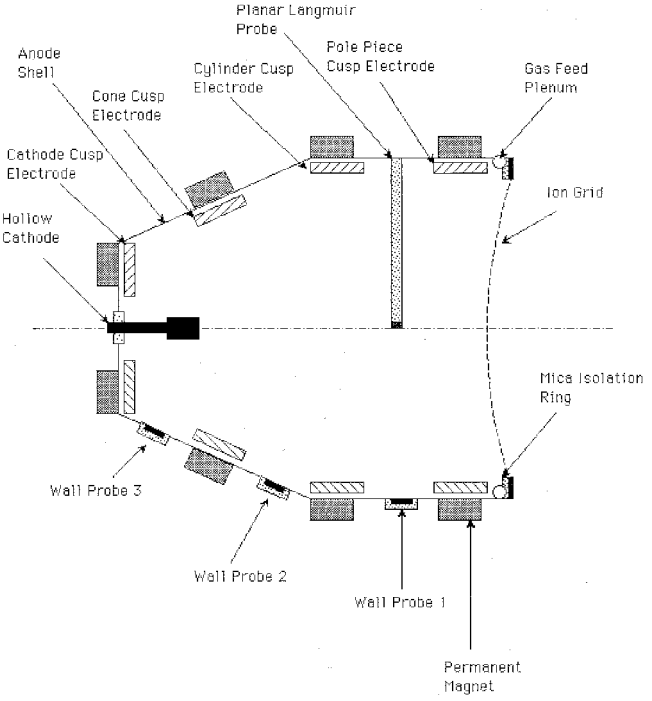

Fig. 1 Eight-cm ion thruster discharge chamber; position of wall ion probes designated by numbers along discharge chamber wall.

with a cylindrical extension, was 9 cm long end to end. A keeperless hollow cathode served as the electron source for the discharge. The discharge chamber was constructed of nonmagnetic stainless steel (0.6 mm thick). Four evenly spaced rare-earth magnet rings of alternating polarity were spot welded via nichrome straps to the outer surface of the discharge chamber to form the ring–cusp magnetic circuit. Located on the inner surface of the discharge chamber at each magnet ring was a 1.27-cm-wide, 0.16-cm-thick stainless-steel ring. The rings are named according to location, as indicated in Fig. 1. Each ring, four in all, was electrically isolated from the anode shell via a ceramic paste and polyimide film sandwich. This insulating material is shadow shielded by the cusp electrode to reduce the likelihood of a conducting layer forming between the ring and the anode shell. The mechanical and electrical connection to each cusp electrode is made via an alumina feedthrough located at the anode shell wall. The current to each cusp electrode and the anode shell was measured via a multimeter. Each cusp electrode and the anode shell could be independently switched into or out of the discharge circuit via single-pole switches. Additional details regarding the 8-cm thruster may be found in Ref. 4.

The xenon gas used to create the plasma enters the discharge chamber through the hollow cathode orifice and a gas feed plenum. For these experiments, the cathode and the gas feed plenum flow rates were each fixed at 1 standard cm^3/min. This flow split is similar to that used the 8-cm thruster study discussed in Ref. 4. The main plenum was oriented in the reverse-feed (directed toward the cathode) configuration. This configuration, which increases the effective discharge chamber length, has been shown to enhance propellant utilization by as much as 5% (see Fig. 1).[4,9]

A single, multiaperture molybdenum grid was used to collect ion current at the exit plane where the thruster's ion acceleration grids would otherwise be located. The bias on this electrode was varied relative to the cathode potential until the collected ion current reached saturation. This ion saturation current represents the maximum ion current available for extraction. The uncertainty in the ion grid current measurements was less than 5%. The ion grid was electrically isolated from the discharge chamber by a 0.5-mm-thick mica ring. The ion grid, which contains 1300 apertures, had a physical open area fraction of 0.18. This open area was designed to simulate the open area fraction to neutrals presented by the screen and accelerator grid combination used during actual beam extraction in the 8-cm engine. Tantalum planar probes, located at the surface of the anode shell midway between each magnet ring, were used to measure ion current to the anode surface area between cusps. These wall probes were electrically isolated from the wall via polyimide film. The position of each probe is designated by numbers 1–3 as shown in Fig. 1. The langmuir probe, which was located midway between the cylinder and pole piece cusp, extended to the centerline of the discharge chamber. The langmuir probe was located roughly 2.0 cm upstream of the ion grid. The component of the magnetic field parallel to the langmuir probe's collection surface was roughly 5×10^{-3} T. The parallel field component at the wall probes was well over 3×10^{-2} T. Both the wall probes and the langmuir probe were disks 0.635 cm in diameter, which corresponded to surface areas of 0.32 cm^2 each.

III. Experimental Results and Discussion

A. Operating Characteristics of the Four-Ring Discharge Chamber

One objective of this study was to analyze the allotment of discharge current to anode surfaces as a function of discharge power. From this information, the effectiveness of the magnetic circuit at confining the plasma could be assessed.

Figure 2 shows a plot of the current distribution to the various cusps and the anode shell. Because the cusp electrodes are of different diameters, the current at each ring is divided by its circumference to remove misleading effects associated with such differences. Here, the anode shell refers to the plenum and all of the surfaces between the cusps. For these tests, the discharge current varied between 1.0 and 2.0 A, which corresponded to measured discharge voltages ranging between 20 and 30 V. As expected most of the electron current collection occurs at the cusps.

It is beneficial to have most of the plasma production occurring near the ion grid. In relation to ion thruster operation, this condition minimizes the power required to produce a given beam for a given flow rate. The cusp current distribution is a rough indicator of the location of the discharge. The discharge tends to be localized in those regions where most of the current is collected. In general, it then follows that to assure discharge localization near the grid, the majority of the discharge current must be collected at the most downstream cusps.[10] In the case of the four-ring thruster, as indicated in Fig. 2, the highest current densities are measured at the cusps in the conical section. Indeed, the higher current densities measured in the conical section suggest that the plasma density is highest there. This tendency to favor plasma production in the conical section as compared to the cylindrical section is most likely due to the close proximity of the cathode cusp and the cone cusp to the cathode (see Fig. 1). This distribution of cusp currents is not consistent with efficient discharge operation as determined in earlier investigations of 30-cm ion thrusters, where most of the discharge current was collected at the

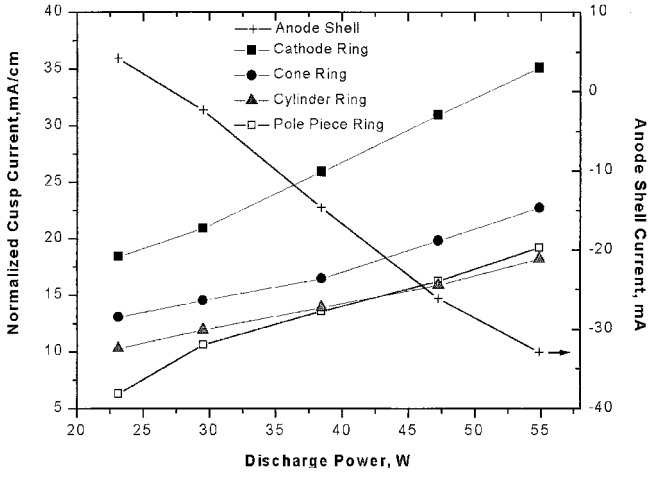

Fig. 2 Normalized current collection at anode cusps and shell as a function of discharge power; negative current value is associated with ion collection.

most downstream cusps.[10,11] The 8-cm discharge chamber's current distribution no doubt contributes to reduced discharge efficiency.

Another interesting point shown in Fig. 2 is the amount of current collected at the anode shell. The net current collected at the shell never exceeded 2% of the total discharge current. The relatively small amount of electron current collected at the anode shell is a consequence of the transverse magnetic field between cusps, which severely limits electron diffusion to the walls. Also note that the current to the anode shell changes polarity from electron dominated to ion dominated as discharge power increases. This change in polarity is due to a relative increase in ion flux to the walls. This polarity change is most likely attributable to an increase in the electron repelling potential at the anode.

The ion wall probes provide direct measurement of the rate at which ions are lost to anode surfaces between cusps (anode shell). For these tests, ion saturation occurred when the probes were biased near cathode potential. The uncertainty in the measured current to the wall probes was less than 5%. Over the power range investigated, ion current density at the wall probes in the conical section was consistently higher than that collected by the cylindrical extension wall probe 1. Using the wall probe data, the average ion current collected at the shell in the conical section and the cylindrical extension was estimated. It was found that the average ion current collected in the conic region was over 40% higher than that collected in the cylindrical extension. This finding is particularly interesting because the magnetic field component parallel to wall probes 2 and 3 in the conical section were, respectively, 35 and 10% higher than that at probe 1 in the cylinder section. The higher ion currents collected at the probe in the conical section are consistent with the presence of a higher density plasma located in that region as suggested by the cusp current density measurements discussed earlier. In this respect, ion loss to the walls appears to be dominated by collection in the conical section.

Extractable ion current as a function of discharge power was determined by biasing the ion grid 20 V below cathode potential to achieve ion saturation. As expected, the ion current increased monotonically with increasing discharge power. A plot of the ion grid current as a function of the discharge current is shown in Fig. 3. Also shown in Fig. 3 is the ratio of the absolute value of the ion grid current to the total discharge current. The current ratio increases with increasing discharge current, which suggests that the discharge electrons are being effectively utilized in the discharge. Additionally, the ratio of ion wall probe current to grid ion current was determined. This ratio, which was found to be roughly constant at each wall probe, suggests that the two ion fluxes are proportional. This well-known finding indicates that the relative rates of ions lost to the wall and at the grid do not change with power.[10,11]

B. Effect of Current Redistribution on Discharge Performance

A series of experiments were undertaken to investigate the effect of externally varying the current allotment at each cusp. This approach is complementary to an earlier investigation in which the potential of electrodes placed between cusps is varied to affect the cusp collection width.[12] In this study, it was found that biasing the intercusp electrodes positive relative to the anode reduced the loss rate of ions to the chamber wall, thereby improving discharge performance. The experiments conducted in this work entail forcing the current to collect at a given cusp combination by floating one or two selected cusp electrodes. For reference, in the baseline configuration no electrodes float. The forced redistribution was expected to give rise to variations in the ion production cost and the overall ion current to the ion grid. Such changes are a consequence of varying the effective anode collection area.[13–15]

For these experiments, the discharge performance was first assessed under conditions where only one cusp electrode was removed from the discharge circuit. In all but one case did floating only one cusp electrode result in a noticeable change in performance. This noticeable change, which resulted in an 8% reduction in ion production costs, occurred when the pole piece electrode was allowed to float. Similar results were observed when this electrode was allowed to float in a 30-cm ion thruster investigation.[11] The discharge could not be sustained with three cusp electrodes floating. Large changes in performance were observed when two of the four cusp electrodes were removed from the discharge circuit and allowed to float. Figures 4a and 4b show the effect of current reallotment on grid ion current and ion production costs (ratio of discharge power to grid ion current) for a number of notable configurations in which two of the four cusp electrodes float. The configuration in which the cone and cathode cusp electrodes floated was not stable, and therefore no data were collected at this condition. Apparently, collection at the cusps in the conical section is necessary for the maintenance of the discharge. For all floating cusp electrode configurations tested, the ion saturation current to the grid increased linearly with increasing discharge power. This finding suggests that plasma density for

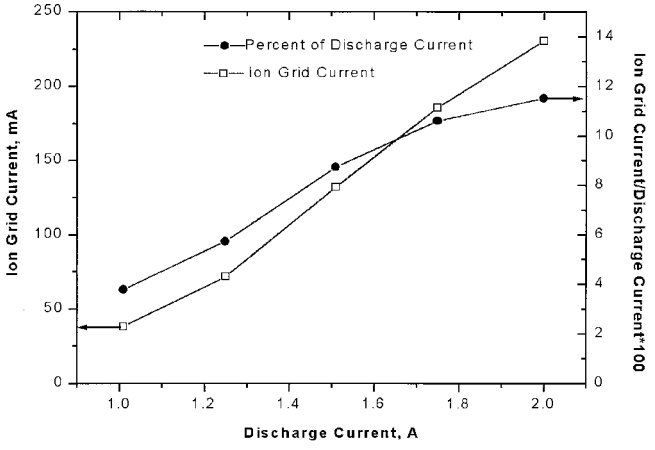

Fig. 3 Ion grid current and ion grid current fraction as a function of discharge current.

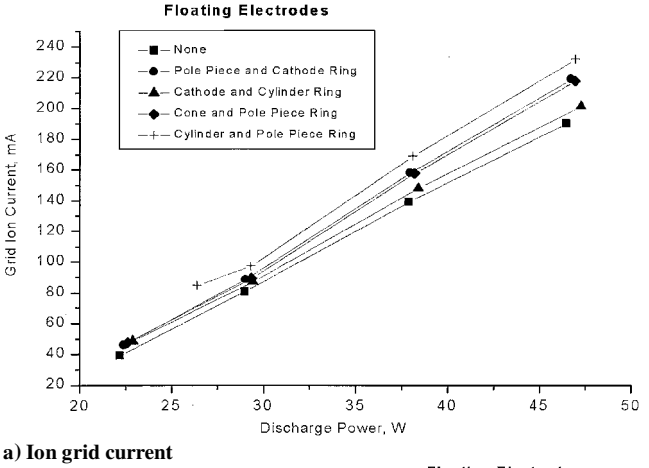

a) Ion grid current

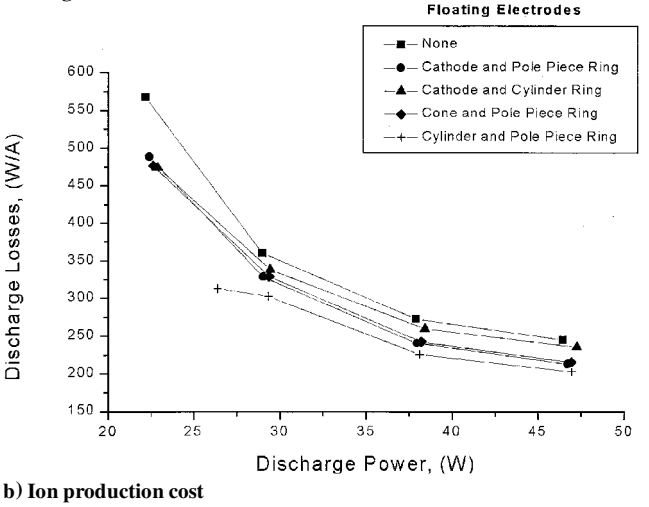

b) Ion production cost

Fig. 4 Floating cusp configurations as a function of discharge power.

all configurations increased linearly with discharge power. Note in Fig. 4b that overall performance improved relative to the baseline (no floating cusps) when two cusps were allowed to float. Ion production costs decreased from nearly 600 W/A to under 225 W/A over the power range investigated. These findings suggest improved ion production near the grid when two cusps float. Best discharge performance was achieved when both the pole piece and the cylinder cusp electrodes float simultaneously. The mechanism behind this improved discharge performance is discussed in Sec. III.C.

Note that those electrode combinations that included the pole piece as a collector were the lowest performers. Because of its proximity to the ion grid, it may be anticipated that variations in current collected at the pole piece cusp should have a measurable effect on ion grid current. Pole piece collection may contribute to the reduction in ion current at the grid. Plasma losses to this cusp may actually deplete the plasma near the grid. Additionally, because the propellant is injected in the vicinity of the pole piece ring, electron cross-field diffusion probably occurs at a more rapid rate there. In this respect, the pole piece cusp may have a parasitic effect on the discharge plasma local to the grid. Again, this reasoning is supported by the noticeable increase in performance when the pole piece electrode is allowed to float alone or float in combination with another cusp.

C. Isolation of the Pole Piece and the Cylinder Ring

Operation with the pole piece and cylinder cusp electrodes floating yielded a significant increase in performance relative to the baseline configuration and the many other cusp electrode configurations tested. The increase in the ion grid current that results from floating the pole piece and cylinder cusp electrodes gives rise to roughly a 20% decrease in ion production costs relative to the baseline configuration at similar discharge powers (see Fig. 4).

To obtain a better understanding of why this configuration performed best, langmuir probe data were acquired to measure trends in the electron temperature and plasma density. The transverse magnetic field component (parallel to probe surface, transverse to diffusion) at the probe was approximately 5.0×10^{-3} T. Though this field strength at the probe surface is significant, the ratio of the Debeye length to Larmor radius is less than one; therefore, basic probe theory was used to analyze the langmuir probe current–voltage characteristic.[16] An average electron temperature was determined from the linear portion of a logarithmic plot of electron current vs probe voltage. Evidence of a second linear region associated with the high-energy primaries was not clearly observed. The absence of the second linear portion in the logarithmic plot is primarily attributed to the elevated pressure in the discharge chamber and a poor signal-to-noise ratio in that region of the IV characteristic. Plasma density was determined from the ion saturation current using the relation:

$$\Gamma_i = 0.61 \cdot n_0 \cdot e \cdot \sqrt{kT_e/M_i} \tag{1}$$

Because ion motion near the ion grid is not severely restricted by magnetic effects ($B < 3.0 \times 10^{-3}$ T), Eq. (1) should also be applicable to current collected there. The electron temperature was used along with the ion saturation current measured at the grid to estimate the ion density local to the grid. The ion density and the electron temperature for a series of operating conditions are shown in Figs. 5a. and 5b. The uncertainties in absolute density measurement and the absolute electron temperature measurement were estimated to be of order 30 and 25%, respectively. As indicated in Figs. 5, the ion density significantly increases when the pole piece and cylinder electrodes float. Additionally, the electron temperature is larger under the floating conditions.

Under floating conditions, the measured increase in electron temperature and plasma density may be the result of enhanced energetic electron confinement, which gives rise to enhanced plasma production. As shown in Fig. 6, the cylinder electrode floats relative to the anode at potentials above the excitation energy of xenon metastables (8.32 eV). The pole piece electrode floats at potentials relative to the anode above the ionization potential of xenon (12 eV). Therefore, the negative potential of the floating cusps has the capacity

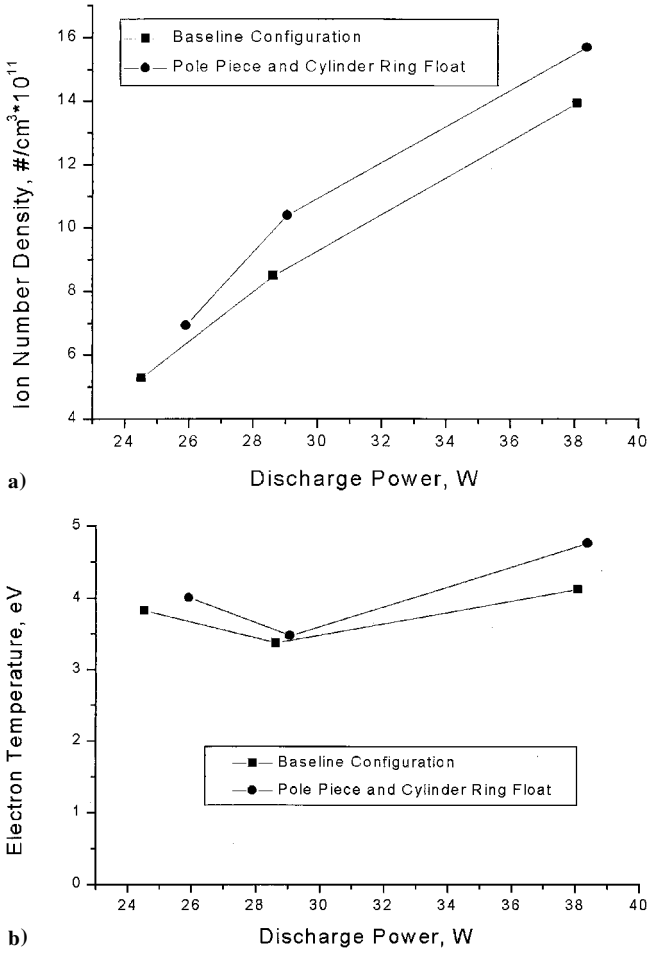

Fig. 5 Variations as functions of discharge power with and without floating cusps in the cylinder section for a) ion number density and b) electron temperature.

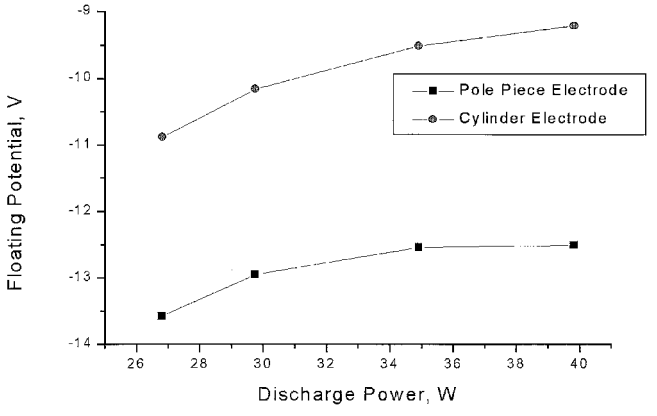

Fig. 6 Variation in the floating potential of the cylinder and pole piece cusp electrodes as a function of discharge power.

to reflect those electrons with energies capable of ionizing xenon either directly by impact ionization or indirectly by ionization of excited xenon metastable states. The negative floating potential is established by the arrival rate of ion and electrons to the electrode and is, therefore, a function of the magnetic field strength at the cusp and the local electron temperature. Thus, the benefit of the floating cusps becomes clear. This reflection mechanism has the effect of increasing the residence time of the hot electrons in the discharge, which in turn increases the likelihood of such electrons undergoing inelastic collisions with neutrals. Additionally, it is likely that this enhanced containment of hot electrons also gives rise to the increase in the measured electron temperature.

It is not surprising that floating the cylinder and pole piece cusp electrodes gives rise to the largest decrease in ion production costs. The electrostatic plugging effect at the floating cusps combined with the strong transverse magnetic field between the cusps give rise to enhanced energetic electron containment in the volume (the cylindrical extension) of the discharge chamber closest to the optics, thereby synergistically enhancing plasma production rates immediately upstream of the ion grid.

Further evidence in support of enhanced plasma production in the region between the floating cusps is provided by the wall probes. The ion current density collected at the wall probe between the two floating electrodes significantly increases when the electrodes are allowed to float. This finding has also been observed in an earlier study where the pole piece cusp was allowed to float.[11] The wall probe ion current distribution also changes when the cusp electrodes float. When the cusp electrodes float, the current density is largest at the wall probe in the cylindrical extension as opposed to wall probe 3, which was the largest under baseline conditions. The ion flux to the wall probes 2 and 3 in the conic section shows reductions in ion flux when the cusps float. Because the ion flux is directly proportional to the plasma density, it may be inferred that the increases in the ion current collected at wall probe 1 are due to increases in plasma density (to first order) in the region. This increase in density in this region also increases the ion flux to the grid. Reductions in current collected at wall probes 2 and 3 may be a consequence shift in the discharge plasma toward the cylindrical extension. Because significantly more electron current flows to the conical section cusps when the cylinder section cusps float, neutral heating in the conical section due to collisions can be expected to increase. Such heating would tend to rarify the gas in this region. The gas rarification would in turn lead to a reduction in plasma density and, thus, a reduction in ion current to the wall probes in the conical section. The reductions in density in the conical section are made up by increased electron collection at the anode shell. The increase in electron current to the anode shell when the cusps in the cylindrical extension float is shown in Fig. 7. The polarity of the shell current changes from ion dominated to electron dominated when the cusp electrodes float. As shown, electron current to the shell increases rapidly initially only to saturate at larger discharge powers. In general, the electron flux to the anode shell is the sum an electric field term and a diffusion term:

$$\Gamma_e = -\mu_e \cdot n_e \cdot E_r - D_\perp \cdot \frac{\partial n_e}{\partial r} \tag{2}$$

The diffusion term, as indicated in Eq. (2), is directly proportional to the electron density gradient. Again, because electron collection at the floating cusps is significantly reduced, the electron density gradient will increase and, thus, drive electrons into the shell. In this regard, the shell plays a larger role in electron collection when the cusps float. This behavior is a direct consequence of anode area-limited collection.

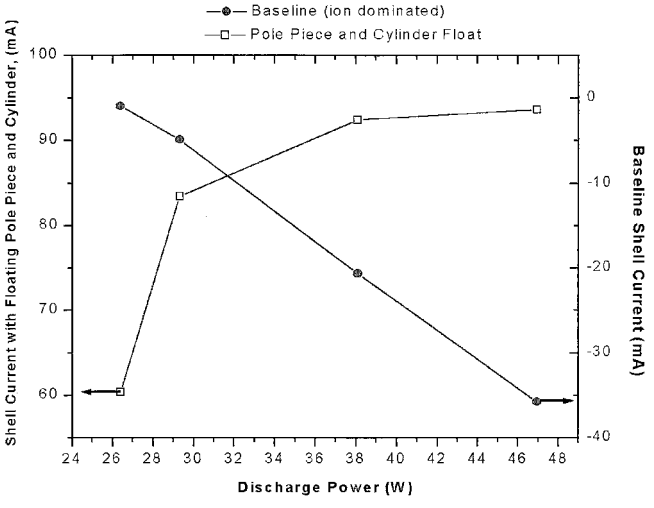

Fig. 7 Variation in current collected by the anode shell with and without cusps in the cylinder section floating; negative currents refer to ion collection.

IV. Conclusion

Discharge plasma properties of an 8-cm ion thruster without beam extraction were investigated using isolated electrodes at the anode cusps, wall ion probes, and a Langmuir probe. As determined from cusp electrode measurements, most of the discharge current was collected at the magnet rings. Less than 2% of the discharge current is collected at the wall surfaces between cusps. Altering the current distribution by floating the cusp electrodes was found to give rise changes in discharge performance. It was found that floating the pole piece and cylinder cusps gave rise to significant increases in performance as measured by reductions in the ion production cost. This increase in performance is believed to be due to enhanced confinement of energetic electrons by the floating potential at the floating cusps. This enhanced confinement increases the ionization efficiency of hot electrons. These findings point to a relatively straightforward way to improve performance of the 8-cm ion thruster.

Acknowledgments

The authors would like to thank James S. Sovey for meaningful discussions regarding this work and technicians Erhard Hartman, Michael R. Pastel, and Ralph A. Jacko for fabrication of hardware used in this investigation.

References

[1]Patterson, M. J., Grisnik, S. P., and Soulas, G. C., "Scaling of Ion Thrusters to Low Power," *Proceedings of the International Electric Propulsion Conference*, IEPC Paper 97-098, Aug. 1998.

[2]Cirri, G. F., Matticari, G., Noci, G., Perrotta, G., Ross, M. F., and Sabbogh, J., "Low Thrust Ion Propulsion: Development Activity at Proel Tecnologie," *Proceedings of the International Electric Propulsion Conference*, IEPC Paper 93-107, Sept. 1993.

[3]Mueller, J., "Thruster Options for Microspacecraft: A Review and Evaluation of Existing Hardware and Emerging Technologies," AIAA Paper 97-3058, July 1997.

[4]Patterson, M. J., "Low Power Ion Thruster Development Status," AIAA Paper 98-3347, July 1998.

[5]Kaufman, H., "Technology of Electron Bombardment Ion Thrusters," *Advances in Electron and Electron Physics*, Vol. 36, Academic Press, San Francisco, 1974, pp. 266–272.

[6]Sovey, J. S., "Improved Ion Containment Using a Ring-Cusp Ion Thruster," *Journal of Spacecraft and Rockets*, Vol. 21, No. 5, 1984, pp. 488–495.

[7]Chen, F., *Introduction to Plasma Physics*, Plenum, New York, 1984, pp. 27–34, 169–175.

[8]Brophy, J. R., "Simulated Ion Thruster Operation Without Beam Extraction," AIAA Paper 90-2655, 1990.

[9]Patterson, M. J., and Rawlin, V. K., "Derated Ion Thruster Design Issues," *Proceedings of the International Electric Propulsion Conference*, IEPC Paper 91-150, Oct. 1991.

[10]Beattie, J. R., and Poeshel, R. L., "Ring Cusp Ion Thrusters," *Proceedings of the International Electric Propulsion Conference*, IEPC Paper 84-71, May 1984.

[11]Beattie, J. R., and Matossian, J. N., "Mercury Ion Thruster Technology," NASA CR-174974, March 1989.

[12]Yoshihiro, A., and Hamantani, C., "Reduction of Plasma Loss to Discharge Chamber Walls in a Ring-Cusp Ion Thruster," *Journal of Propulsion*, Vol. 3, No. 1, 1987, pp. 90, 91.

[13]Goede, A. P. H., and Green,T. S., "Operation Limits of Multipole Ion Sources," *Physics of Fluids*, Vol. 25, No. 10, 1982, pp. 1797–1810.

[14]Goebel, D. M., "Ion Source Discharge Performance and Stability," *Physics of Fluids*, Vol. 25, No. 6, 1982, pp. 1093–1102.

[15]Horiike, H., Akiba, M., Ohara, Y., Okumura, Y., and Tanaka, S., "Cusp Width and Power Flow Study at a High Power Magnetic Multipole Source," *Physics of Fluids*, Vol. 30, No. 10, 1987, pp. 3268–3275.

[16]Swift, J. D., and Schwar, M. J. R., *Electrical Probes for Plasma Diagnostics*, Iliffe, New York, 1969, Chap. 1, pp. 1–13.